

Understanding Ammonia Oxidation on Transition Metals

Third Annual ECS Guelph Young Researcher Symposium

Leanne D. Chen

August 7, 2025

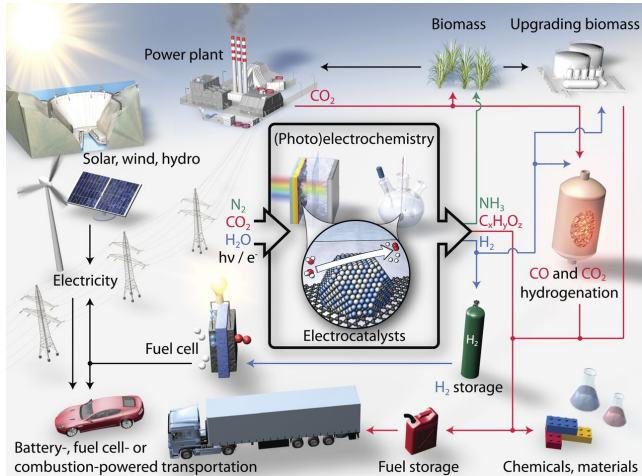
University of Guelph

UNIVERSITY OF
GUELPH

**College of Computational,
Mathematical, and Physical Sciences**

Electrochemical Technology Centre

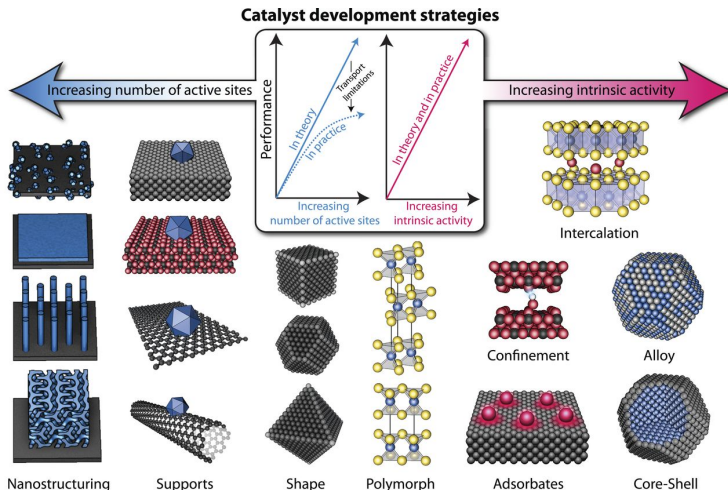
The Energy Transformation Challenge



mechanistic understanding
↓
stable, active, and selective
electrocatalysts

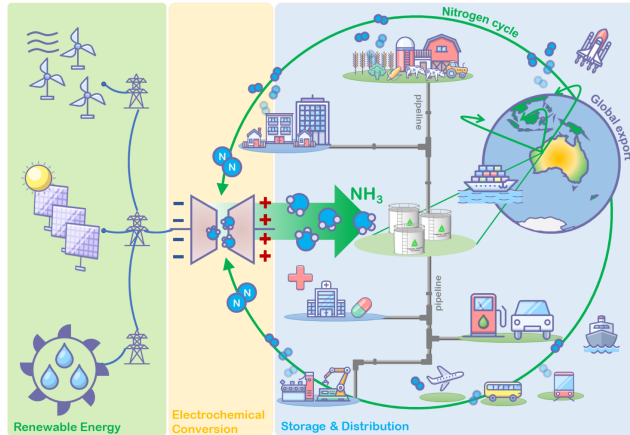
Seh, Z. W.; Kibsgaard, J.; Dickens, C. F.; Chorkendorff, I.; Jaramillo, T. F. *Science* 2017, 355, eaad4998.

Strategies to Improve Electrocatalysts



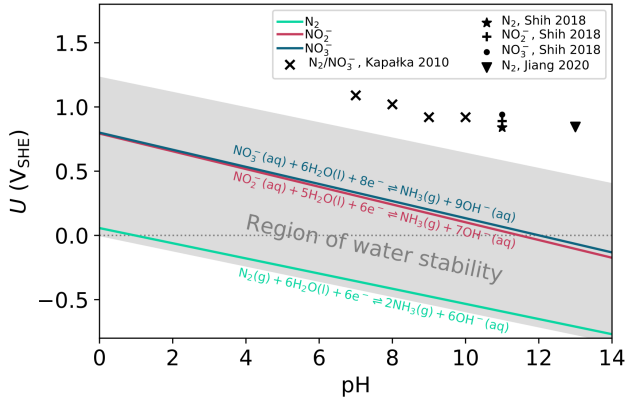
Seh, Z. W.; Kibsgaard, J.; Dickens, C. F.; Chorkendorff, I.; Jaramillo, T. F. *Science* 2017, 355, eaad4998.

The Ammonia Economy



MacFarlane, D. R.; Cherepanov, P. V.; Choi, J.; Suryanto, B. H. R.; Hodgetts, R. Y.; Bakker, J. M.; Ferrero Vallana, F. M.; Simonov, A. N. *Joule* 2020, 17, 1186–1205.

Ammonia Oxidation Pourbaix Diagram



Choueiri, R. M.; Tatarchuk, S. W.; Klinkova, A.; Chen, L. D. *Electro. Chem. Sci. Adv.* 2021, e2100142.

The Computational Hydrogen Electrode (CHE)

Our reference is the half-reaction



This reaction is defined to be at equilibrium at $U = 0$ V, $\text{pH} = 0$, and $p_{\text{H}_2} = 101325$ Pa. Then we can equate the chemical potentials of the proton-electron pair with half that of the gas-phase H_2 molecule

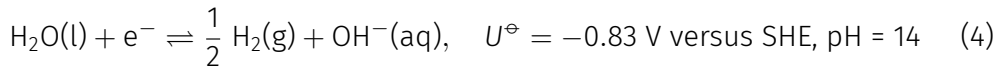
$$\mu_{\text{H}^+(\text{aq})} + \mu_{\text{e}^-} = \frac{1}{2} \mu_{\text{H}_2(\text{g})} \quad (2)$$

Additional terms are added to include the effects of pH and potential shifts

$$\mu_{\text{H}^+(\text{aq})}([\text{H}^+]) + \mu_{\text{e}^-}(U) = \frac{1}{2} \mu_{\text{H}_2(\text{g})} + RT \ln \left(\frac{\sqrt{p_{\text{H}_2}}}{[\text{H}^+]} \right) - eU \quad (3)$$

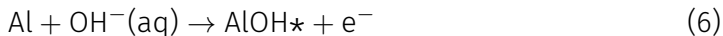
Nørskov, J.K.; Rossmeisl, J.; Logadottir, A.; Lindqvist, L.; Kitchin, J. R.; Bligaard, T.; Jónsson, H. *J. Phys. Chem. B* **2004**, *108*, 17886–17892.

Applying the CHE in Alkaline Conditions



$$\mu_{\text{OH}^-(\text{aq})} - \mu_{\text{e}^-} = \mu_{\text{H}_2\text{O}(\text{l})} - \frac{1}{2} \mu_{\text{H}_2(\text{g})} + RT \ln \left(\frac{\sqrt{p_{\text{H}_2}} [\text{OH}^-]}{a_{\text{H}_2\text{O}(\text{l})}} \right) - (0.83 + eU) \quad (5)$$

To calculate the energy change of an adsorption step

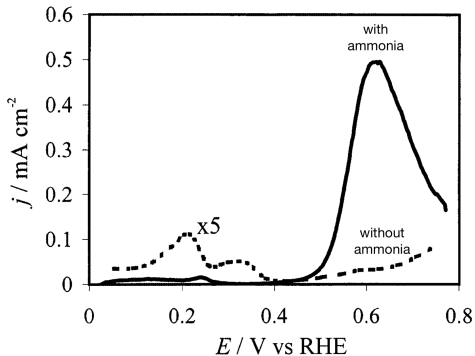


We have

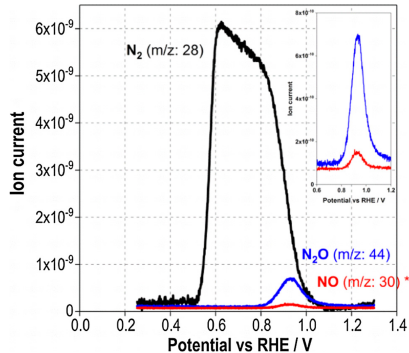
$$\Delta G = G_{\text{AlOH}^*} - G_{\text{Al}} - \left[\mu_{\text{H}_2\text{O}(\text{l})} - \frac{1}{2} \mu_{\text{H}_2(\text{g})} + RT \ln \left(\frac{\sqrt{p_{\text{H}_2}} [\text{OH}^-]}{a_{\text{H}_2\text{O}(\text{l})}} \right) - (0.83 + eU) \right] \quad (7)$$

Chen, L. D.; Nørskov, J. K.; Luntz, A. C. *J. Phys. Chem. Lett.* **2014**, *119*, 19660–19667.

Ammonia Oxidation on Pt

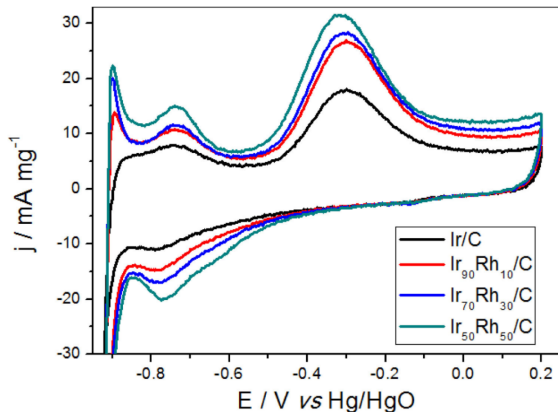


de Voys, A. C. A.; Koper, M. T. M.; van Santen, R. A.; van Veen, J. A. R.
Electroanal. Chem. **2001**, *506*, 127-137.



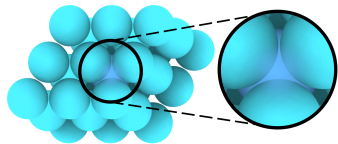
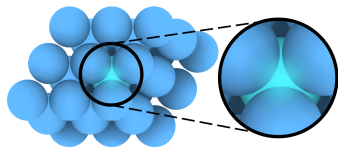
Katsounaros, I.; Figueiredo, M. C.; Calle-Vallejo, F.; Li, H.; Gewirth, A. A.; Marković, N. M.; Koper, M. T. M. *J. Catal.* **2018**, *359*, 82-91.

Ammonia Oxidation on Ir-Rh Alloys

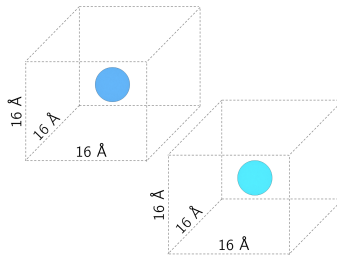


Silva, J. C. M.; Assumpção, M. H. M. T.; Hammer, P.; Neto, A. O.; Spinacé, E. V.; Baranova, E. A. *ChemElectroChem* 2017, 17, 1101–1107.

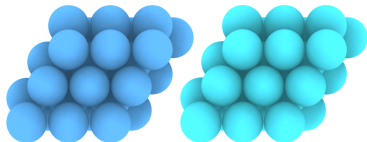
Quantifying Ir-Rh Interactions



Ir-Rh/Rh-Ir

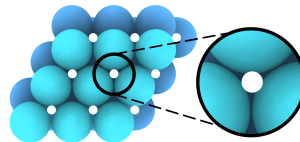


Ir(g) and Rh(g)



Ir

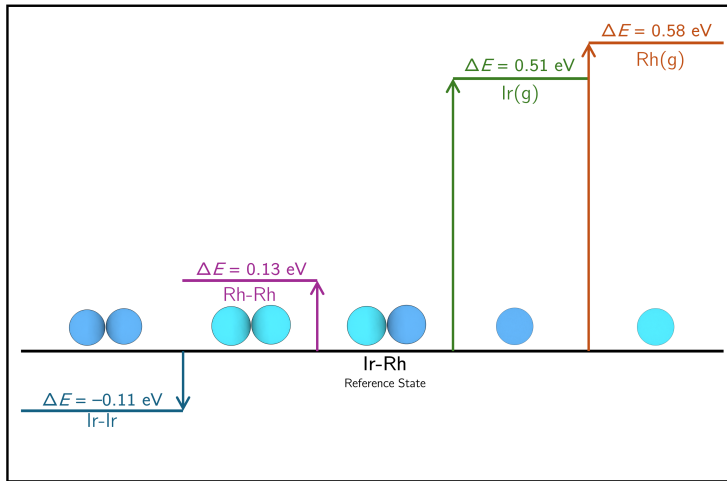
Rh



Placeholder H

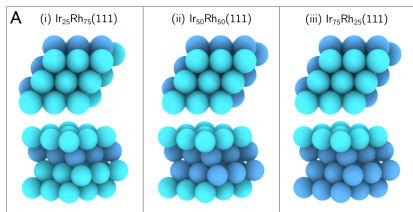
Laframboise, B. J. R.; Johnston, S. J.; Chen, L. D. *ChemCatChem* 2025, 17, e202401177.

Quantifying Ir-Rh Interactions

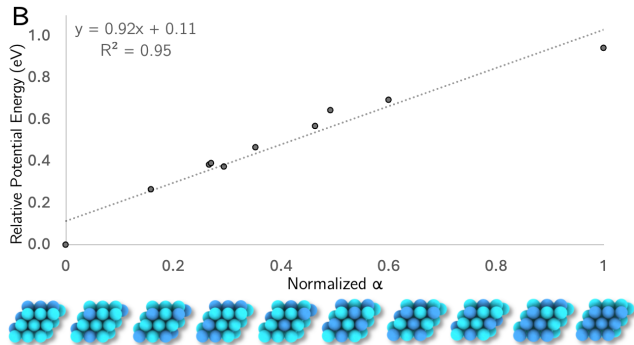


Laframboise, B. J. R.; Johnston, S. J.; Chen, L. D. *ChemCatChem* 2025, 17, e202401177.

Quantifying Ir-Rh Interactions

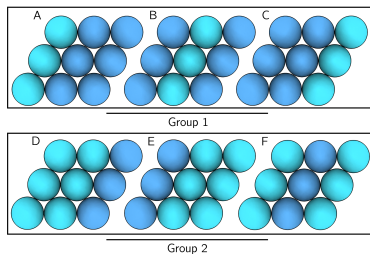


$$\alpha = \sum_{i=1}^N \sum_{j=1}^{12} E_{ij} \quad (8)$$



$$\text{Normalized } \alpha_n = \frac{\alpha_n - \text{Min}(\alpha)}{\text{Max}(\alpha) - \text{Min}(\alpha)} \quad (9)$$

Accounting for Configurational Entropy



$$n_1 = n_2 = n_{\text{elements}}^r = 3^2 = 9 \quad (10)$$

$$n_{\text{layers}} = \binom{4}{2} = 6 \quad (11)$$

$$n_{\text{total}} = n_1 \cdot n_2 \cdot n_{\text{layers}} = 9 \cdot 9 \cdot 6 = 486 \quad (12)$$

Group 1 Layers	Group 2 Layers	Layer Ordering
9 states	9 states	6 states
A,A	D,D	G1,G1,G2,G2
B,A	E,D	G1,G2,G1,G2
C,A	F,D	G2,G1,G2,G1
A,B	D,E	G2,G2,G1,G1
A,C	D,F	G1,G2,G2,G1
B,B	E,E	G2,G1,G1,G2
B,C	E,F	
C,B	F,E	
C,C	F,F	

Laframboise, B. J. R.; Johnston, S. J.; Chen, L. D. *ChemCatChem* 2025, 17, e202401177.

Accounting for Configurational Entropy

Group	Ir Count	Rh Count	Number of States
G ₀	0	9	1
G ₁	1	8	9
G ₂	2	7	36
G ₃	3	6	84
G ₄	4	5	126
G ₅	5	4	126
G ₆	6	3	84
G ₇	7	2	36
G ₈	8	1	9
G ₉	9	0	1

To maintain the 1:1 ratio of Ir and Rh, only combinations of layers with indices that sum up to 18 are considered.

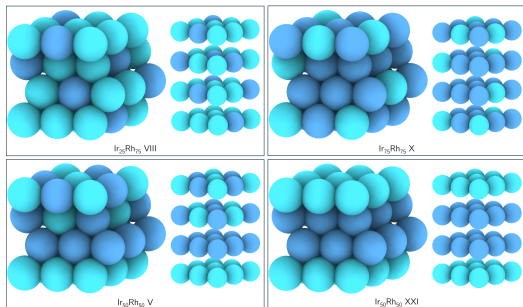
For example, the combination [G₄, G₁, G₆, G₇] is valid, however, the combination [G₈, G₅, G₃, G₉] is not.

$$n_i = \binom{9}{n_{\text{Ir}}} \quad (13)$$

$$n_{\text{total}} = \prod_{i=1}^4 n_i \quad (14)$$

Using Python, it was found that there are 670 valid combinations for a 1:1 ratio of Ir and Rh. Then, taking into account the number of possible states for each group, we end up with a total of 9,075,135,300 configurations, which is equal to $\binom{36}{18}$.

Accounting for Configurational Entropy

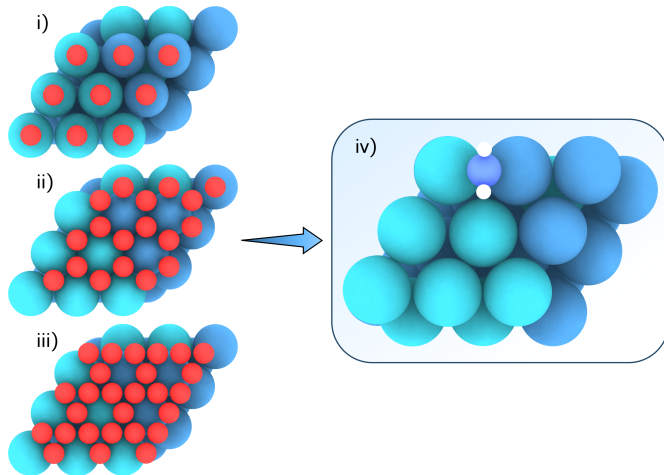


$$S = k_B \ln \Omega \quad (15)$$

Alloy Index	Number of States	$-TS_{\text{config}}$ (eV)
I	1	0
IV	1	0
II	7056	-0.228
III	7056	-0.228
V	15876	-0.248
VI	15876	-0.248
VII	381024	-0.330
X	2286144	-0.376
VIII	2286144	-0.376
IX	3919104	-0.390

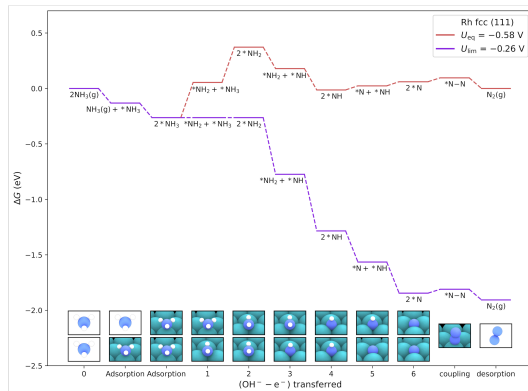
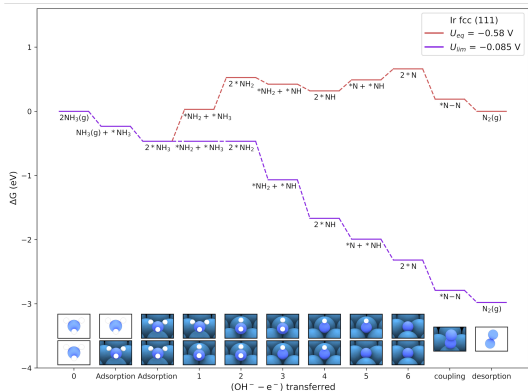
Laframboise, B. J. R.; Johnston, S. J.; Chen, L. D. *ChemCatChem* 2025, 17, e202401177.

Site Testing on Alloy Surfaces



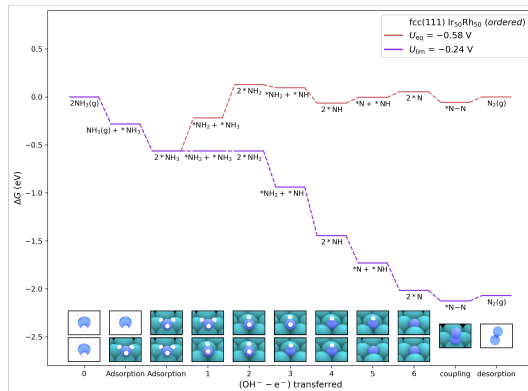
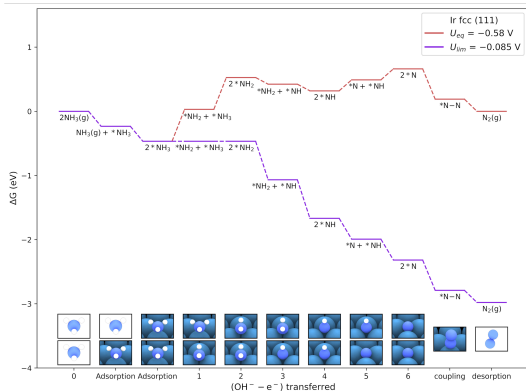
Laframboise, B. J. R.; Johnston, S. J.; Chen, L. D. *ChemCatChem* 2025, 17, e202401177.

N₂ Formation on Pure Ir and Rh

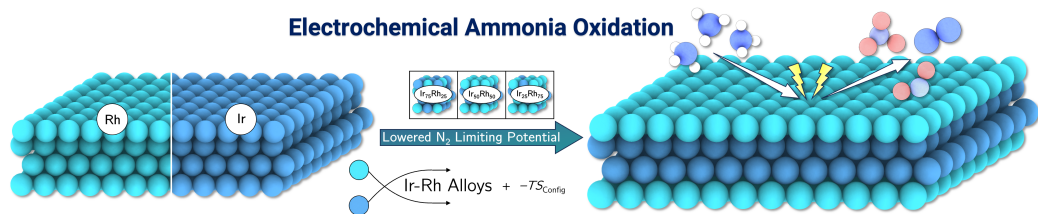


Laframboise, B. J. R.; Johnston, S. J.; Chen, L. D. *ChemCatChem* 2025, 17, e202401177.

N₂ Formation Is Favoured on 50:50 Ir-Rh Alloy

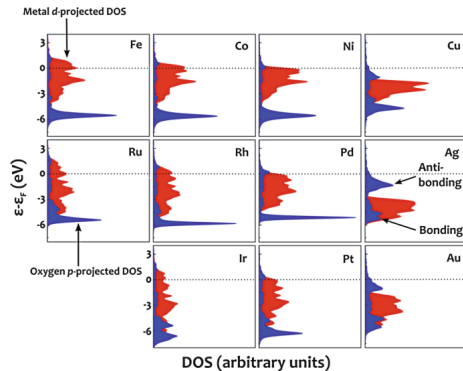
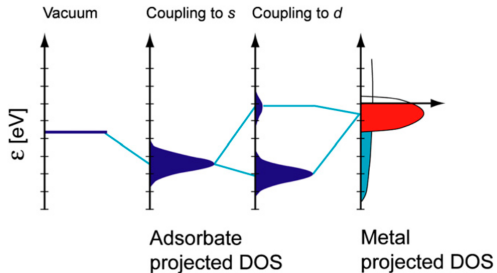


Laframboise, B. J. R.; Johnston, S. J.; Chen, L. D. *ChemCatChem* 2025, 17, e202401177.



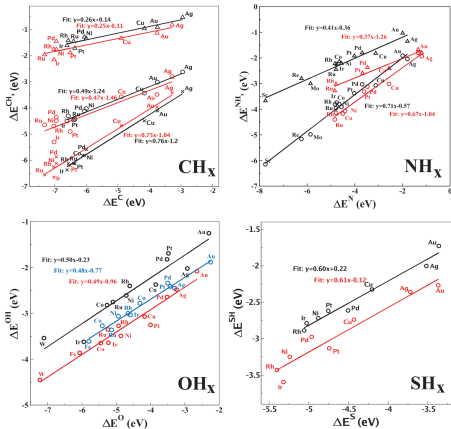
Laframboise, B. J. R.; Johnston, S. J.; Chen, L. D. *ChemCatChem* 2025, 17, e202401177.

The *d*-band Model



Nørskov, J. K.; Studt, F.; Abild-Pedersen, F.; Bligaard, T. *Fundamental Concepts in Heterogeneous Catalysis*; John Wiley & Sons, 2014.

Scaling Relations

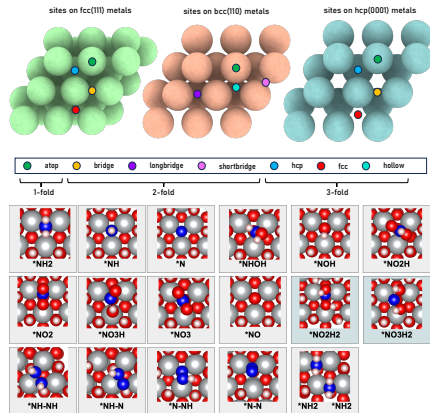


Abild-Pedersen, F.; Greeley, J.; Studt, F.; Rossmeisl, J.; Munter, T. R.; Moses, P. G.; Skúlason, E.; Bligaard, T.; Nørskov, J. K. *Phys. Rev. Lett.*; 2007, 99, 016105.

Calculation Details

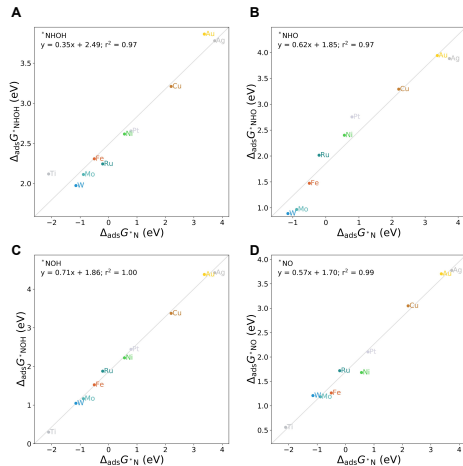
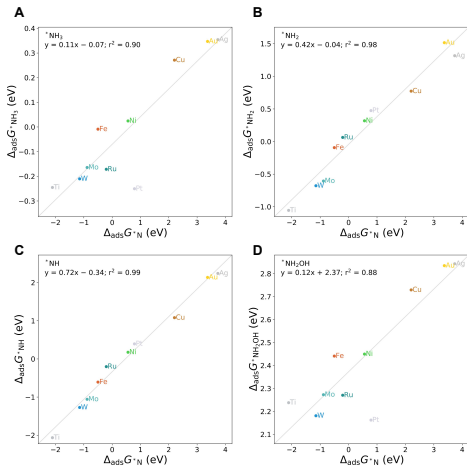
: reference metals
 : test metals
 : excluded species

3 IIIB	4 IVB	5 VB	6 VIB	7 VIIB	8 VIIIB	9 VIIIB	10 VIIIB	1 IB	1 IIB
21 Sc	22 Ti	23 V	24 Cr	25 Mn	26 Fe	27 Co	28 Ni	29 Cu	30 Zn
39 Y	40 Zr	41 Nb	42 Mo	43 Tc	44 Ru	45 Rh	46 Pd	47 Ag	48 Cd
57 La	72 Hf	73 Ta	74 W	75 Re	76 Os	77 Ir	78 Pt	79 Au	80 Hg
89 Ac	104 Rf	105 Db	106 Sg	107 Bh	108 Hs	109 Mt	110 Ds	111 Rg	112 Cn



Choueiri, R. M.; Tatarchuk, S. W.; Parker, O. G.; Cooper, W. M.; Chen, L. D. *Catal. Today* 2025, 448, 115179.

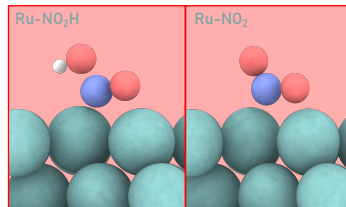
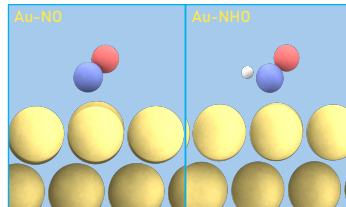
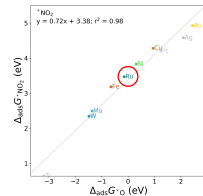
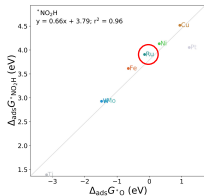
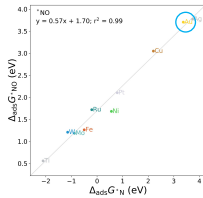
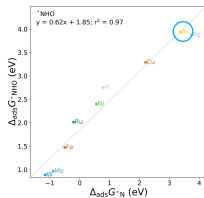
Scaling Relations for Ammonia Oxidation Intermediates



Monodentate and Bidentate Adsorbates

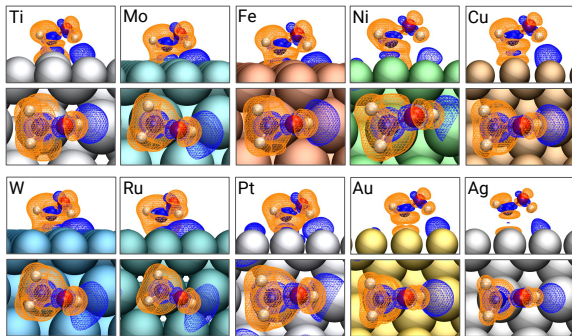
consistent with N-scaling (monodentate) : ■

consistent with O-scaling (bidentate) : ■

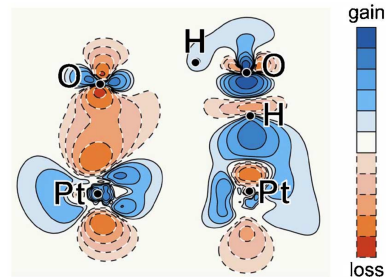


Choueiri, R. M.; Tatarchuk, S. W.; Parker, O. G.; Cooper, W. M.; Chen, L. D. *Catal. Today* 2025, 448, 115179.

Adsorbate-Surface Hydrogen Bonding

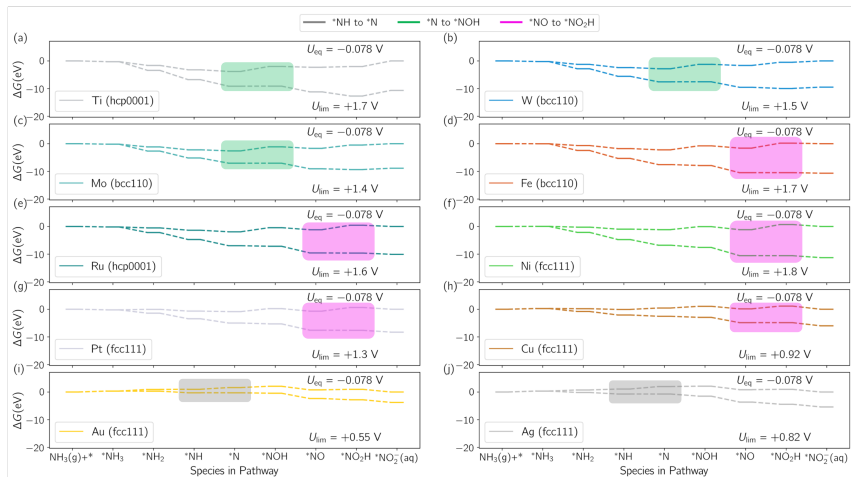


Choueiri, R. M.; Tatarчук, S. W.; Parker, O. G.; Cooper, W. M.; Chen, L. D. *Catal. Today* **2025**, *448*, 115179.



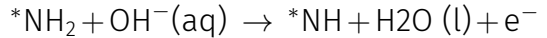
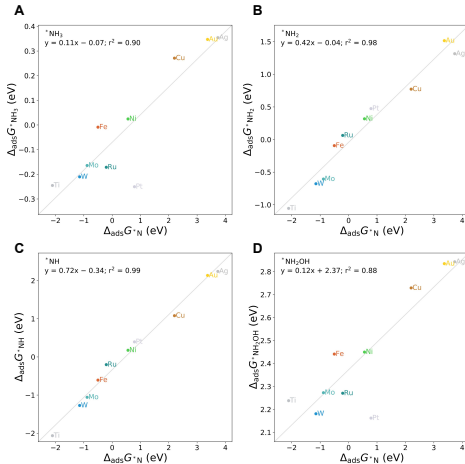
Ogasawara, H.; Brena, B.; Nordlund, D.; Nyberg, M.; Pelmenschikov, A.; Pettersson, L. G. M.; Nilsson, A. *Phys. Rev. Lett.* **2002**, *89*, 276102.

Microkinetic Modelling

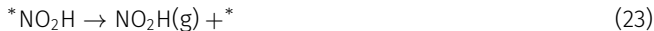
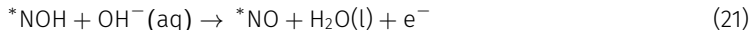
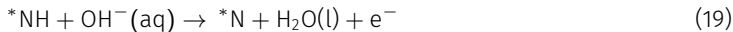
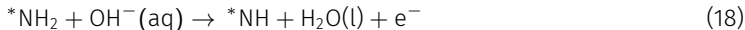
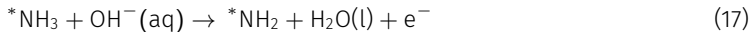


Choueiri, R. M.; Tatarchuk, S. W.; Parker, O. G.; Cooper, W. M.; Chen, L. D. *Catal. Today* 2025, 448, 115179.

Microkinetic Modelling



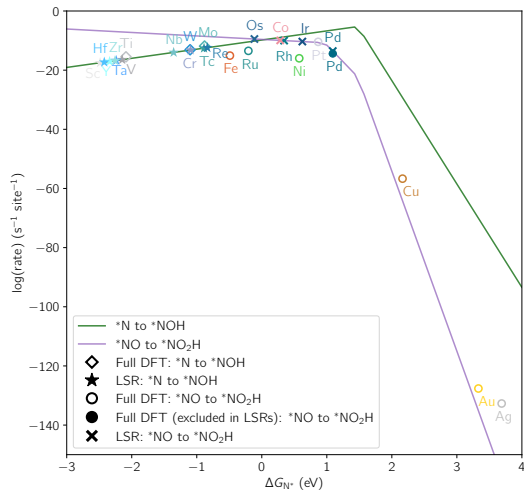
$$\begin{aligned} \Delta_r G(pH, U) = & (m_{^*NH} - m_{^*NH_2}) \Delta_{ads} G_{^*N} \\ & + (b_{^*NH} - b_{^*NH_2}) \\ & + 0.5G_{H_2(g)} - eU - 0.65 \text{ eV} \end{aligned}$$



$$r = \frac{k_B T}{h} e^{\frac{-E_a(\text{RDS})}{k_B T}} [\text{NH}_3][\text{OH}^-]^4 K_1 K_2 K_3 K_4 \theta_* (1 - \gamma_{\text{eq}}) \quad (24)$$

Choueiri, R. M.; Tatarчук, S. W.; Parker, O. G.; Cooper, W. M.; Chen, L. D. *Catal. Today* **2025**, *448*, 115179.

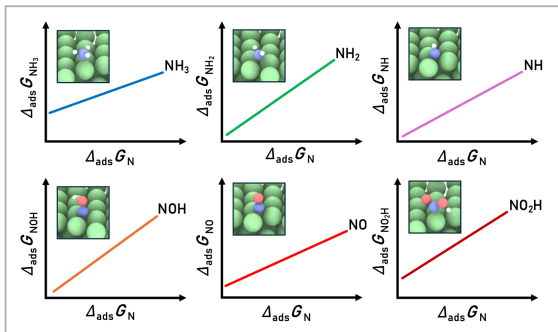
Microkinetic Modelling



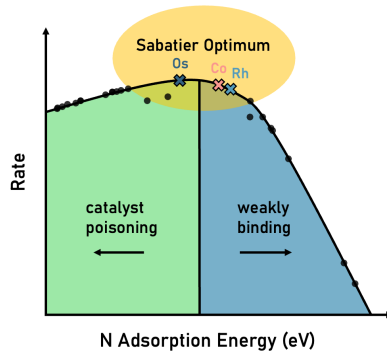
Choueiri, R. M.; Tatarchuk, S. W.; Parker, O. G.; Cooper, W. M.; Chen, L. D. *Catal. Today* 2025, 448, 115179.

Ammonia Oxidation Scaling Relations Summary

Linear Scaling Relations for NO_xH_y

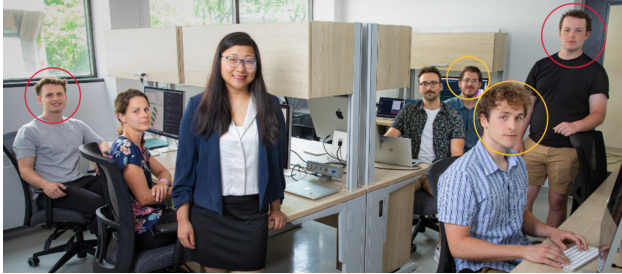


AOR Sabatier Plot for NO_2^- Formation



Choueiri, R. M.; Tatarchuk, S. W.; Parker, O. G.; Cooper, W. M.; Chen, L. D. *Catal. Today* 2025, 448, 115179.

Acknowledgements



Dr. R. Choueiri



O. Parker

Ir-Rh Alloy Work and Scaling Relations Work



Digital Research
Alliance of Canada

Alliance de recherche
numérique du Canada

Acknowledgements



Dr. J. Zhou*
LOHCs (13:15)



B. Laframboise
Pt Alloys (16:01)



B. Paget
Ni Oxide (16:22)

*Jacek Lipkowski Award Lecture

Acknowledgements

Thank you to Jonathan Quintal and Prof. Aicheng Chen
for organizing this Symposium!